applied sciences

MDPI

*Article*

# Time-Series InSAR Deformation Monitoring of High Fill *Characteristic* Canal of South–North Water Diversion Project in China

**Hui Liu [1,2,3,4], Wenfei Zhao [1,*], Zhen Qin [2], Tiesheng Wang [1], Geshuang Li [5] and Mengyuan Zhu [1]**

[1] College of Surveying and Geo-Information, North China University of Water Resources and Electric Power, Zhengzhou 450046, China
[2] Key Laboratory of Ecological Environment Protection of Space Information Application of Henan, Zhengzhou 450046, China
[3] Collaborative Innovation Center of Geo-Information Technology for Smart Central Plains, Zhengzhou 450015, China
[4] Key Laboratory of Spatiotemporal Perception and Intelligent Processing, Ministry of Natural Resources, Zhengzhou 450015, China
[5] Zhengzhou Communications Planning Survey & Design Institute, Zhengzhou 450001, China
* Correspondence: wfzhao@stu.ncwu.edu.cn; Tel.: +86-1771-984-4257

**Abstract:** The Middle Route of the South–North Water Diversion Project has changed the water resources pattern in China. As advanced equipment for the country, it is responsible for the water supply "lifeline" of Beijing, Tianjin, Hebei, Henan, etc. Ensuring its safe operation is a top priority to promote social stability and coordinated economic development between the North and the South. Used persistent scatterer interferometric synthetic aperture radar (PS-InSAR) technology to monitor the deformation of the high fill characteristic canal in Wenzhuang Village, Ye County, during the period from October 2016 to June 2017 for the South–North Water Diversion Project showed that there was significant deformation on the 1 km-long slope of the east bank of the canal, with the maximum deformation volume reaching 36 mm. Through the comparison and verification with the second order leveling data, there are more than 87% of the root mean square error of both less than ±2 mm. The correlation coefficient is 0.96, and the two were highly consistent in deformation trends and values. Through the vertical and cross-sectional analysis of the canal's east bank and four key monitoring sections, it was found that the east bank of the canal presents overall uneven subsidence, and the closer the canal is to the water, the greater the canal deformation, and vice versa. Further comparison of the PS-InSAR deformation results of the canal from October 2016 to February 2018 proves that this technology cannot only monitor the subsidence range and rate of the South–North Water Diversion canal but also accurately identify the subsidence sequence of the east and west banks. It can provide reliable technical support for the safety monitoring and disaster prevention of the South–North Water Diversion canal characterized by high fill and deep excavation.

**Keywords:** South–North Water Diversion Project; time-series InSAR; deformation monitoring; high fill



**Citation:** Liu, H.; Zhao, W.; Qin, Z.; Wang, T.; Li, G.; Zhu, M. Time-Series InSAR Deformation Monitoring of High Fill *Characteristic* Canal of South–North Water Diversion Project in China. *Appl. Sci.* **2023**, *13*, 6415. https://doi.org/10.3390/app13116415

Academic Editor: Nathan J Moore

Received: 4 March 2023
Revised: 17 May 2023
Accepted: 23 May 2023
Published: 24 May 2023



## 1. Introduction

In China, The Middle Route of the South–North Water Diversion Project, which is the "lifeline" for water supply to Beijing, Tianjin, Hebei, and Henan, has been operating uninterruptedly and overloaded for more than seven years. Since its official opening on 12 December 2014, supplying more than 50 billion cubic meters of water to the north and directly benefited 140 million people which is the source of water for 70–80% of Beijing and 100% of Tianjin. It has not only relieved the water shortage in large and medium-sized cities along the route but also greatly improved the ecology of rivers along the route. It created opportunities and space for economic restructuring and industrial transformation. It is of

great significance for safety monitoring [1–3]. However, the country's heavy weapons are "overdue" and "over the standard service", so the risk of failure cannot be fully controlled and security monitoring is significant.

At present, the safety monitoring of the South–North Water Diversion Project is mainly based on precision leveling measurement, GNSS (Global Navigation Satellite System) measurement and sensors installed inside the project. These methods have low spatial sampling density and can only obtain local point settlement. It is difficult to grasp the information of deformation at non-measurement points and the continuous deformation trend of the dam as a whole [4–6]. At the same time, the cost of human and material resources is high. The first two methods require the measurement personnel to enter the deformation area, which increases the danger; the latter method's sensors are difficult to maintain and will gradually lose sensitivity and even efficacy with the operation of the dam. There is an urgent need for a new method to measure the deformation of dams and surrounding landscapes in a large area at a low cost. InSAR (Interferometric Synthetic Aperture Radar) technology with all-day, all-weather, strong penetration, and surface domain deformation monitoring capability provides a new idea for wide-scale, high-precision safety monitoring of the South–North Water Diversion Project [7–12]. The PS-InSAR (Persistent Scatterer Interferometric Synthetic Aperture Radar) technique proposed by Ferretti et al. [13] can obtain millimeter-level deformation monitoring accuracy. The InSAR technique has been promoted in algorithm research [14–21], surface subsidence [22–24], disaster warning [25–28], permafrost deformation [29–31], and other fields have made significant breakthroughs. In recent years, InSAR technology has also been widely used in water conservancy project safety monitoring. Dong J et al. [32] first conducted a deformation census of the Middle Route of the South–North Water Diversion Project using Sentinel-1 images. Then, high-resolution images and level data were used to focus on analyzing the deformation results in areas, such as the Jiaozuo and Tianjin sections, verifying the feasibility of InSAR technology in long-span linear water conservancy projects. Wang N et al. [33] used PS-InSAR technology to monitor the Middle Route of the South–North Water Diversion Project in Henan Province. At the same time, it has found 20 deformation areas and 7 suspected deformation areas. Those studies further proved the effectiveness of InSAR technology applied to the spatial and temporal variation characteristics of the South–North Water Diversion Project Canal. Ma C et al. [34] used ENVISAT ASAR images and the D-InSAR (Differential Interferometric Synthetic Aperture Radar) technique to obtain the deformation monitoring results of the northern section of the South–North Water Diversion Project. It showed that the main reason for the poor stability of this section is the influence of geological and tectonic activities and urban surface subsidence. Zhang Y et al. [35] used SBAS-InSAR (Small Baseline Subsets Interferometric Synthetic Aperture Radar) technique to refine the analysis of the swelling soil area of the South–North Water Diversion Project. It showed that the settlement of the canal section was highly correlated with rainfall, soil moisture, and other factors.

In this paper, for the characteristics of high fill, deep excavation, and large scale of the South–North Water Diversion Project. The PS-InSAR technique was used to obtain the overall deformation results of the high-fill section of Wenzhuang Village in Ye County of the Middle Route of the South–North Water Diversion Project. At the same time, successfully inversion the spatial and temporal variation characteristics of the east and west banks of the canal. Through the comparison and verification of the second-order leveling data. The feasibility and effectiveness of the time-series InSAR technology for the safety monitoring of the high-fill canal of the South–North Water Diversion Project have been proved.

## 2. Materials and Methods

### *2.1. Study Area*

The Middle Route of the South–North Water Diversion Project originates from Danjiangkou Reservoir in Nanyang and extends to Beijing at the end, with a total length of 1432 km. South-to-North Water Diversion Project as a large open-air water conservancy project. It contains inverted siphons, drainage culverts, crossings, bridges, and other water

conservancy projects. At the same time, it crosses the swelling soil area of about 368 km, and the swelling soil will affect the stability of the slope of the canal when it swells with water or loses water and shrinks. Therefore, the Middle Route of the South–North Water Diversion Project has buried second-order leveling benchmarks at intervals during the construction period. Deformation monitoring is important routine work. In this paper, PS-InSAR technology is used to monitor the deformation of the slope of the high-fill canal from pile 210 + 130 to pile 211 + 750 in Wenzhuang Village, Ye County, Middle Route of the South–North Water Diversion Project (Figure 1). It can provide technical support for the safety hazard identification of the South–North Water Diversion Project Canal.

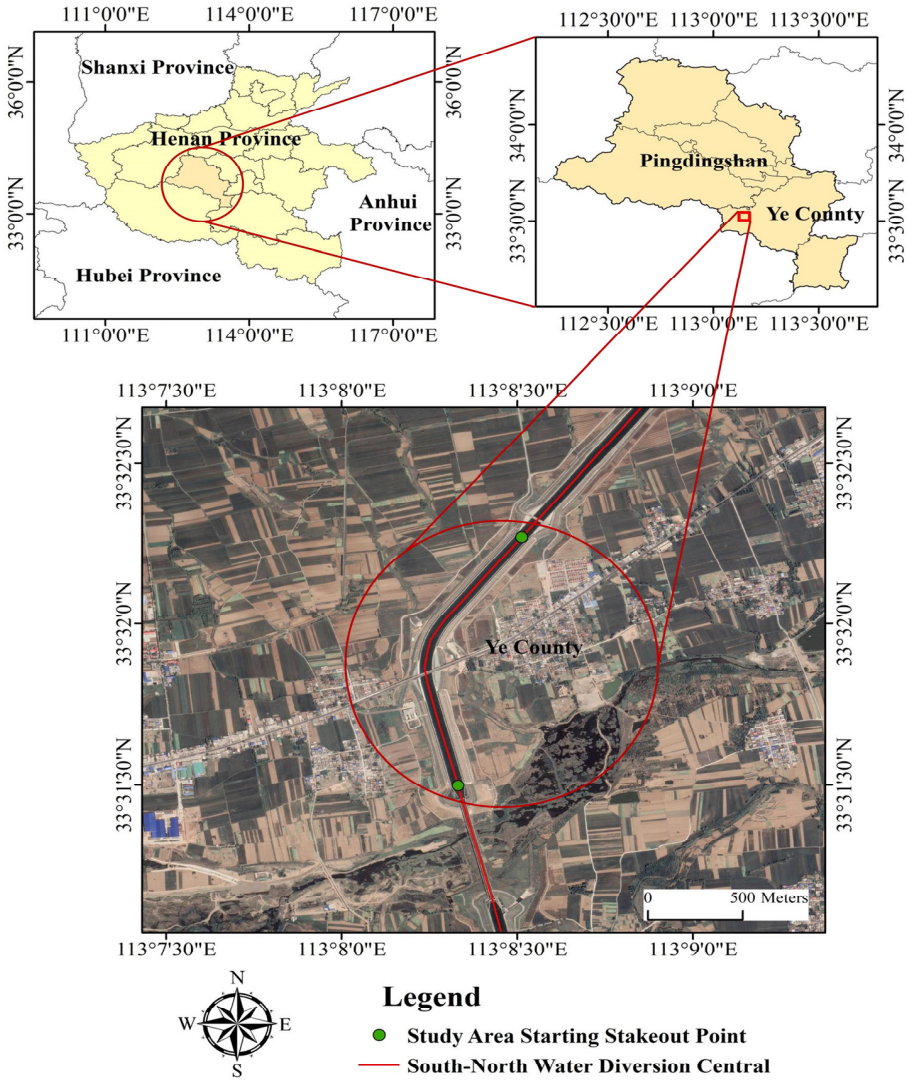


**Figure 1.** Location of the study area.

### *2.2. Data*

In this paper, 23 Sentinel-1A SAR images were used from October 2016 to June 2017 for deformation monitoring of the high-fill canal in Wenzhuang Village, Ye County of the Middle Route of the South–North Water Diversion Project. The image acquired on 30 January 2017 was selected as the master image, and the rest images were used as slave images for subsequent alignment, interference, and inversion processing with the master image. The image spatial and temporal baseline parameters are shown in Table 1. To improve the accuracy of monitoring results, 30 m SRTM DEM (Shuttle Radar Topography Mission Digital Elevation Model) was selected as the reference data for topographic phase removal in InSAR processing (Figure 2).

**Table 1.** Baseline parameter of Sentinel-1A SAR images.

| Date | Vertical Baseline/m | Time Baseline/d |
|---|---|---|
| 2016-10-02 | 44.6939 | −120 |
| 2016-10-14 | 39.6777 | −108 |
| 2016-10-26 | −14.6982 | −96 |
| 2016-11-07 | −45.9389 | −84 |
| 2016-11-19 | −47.9464 | −72 |
| 2016-12-01 | 59.9997 | −60 |
| 2016-12-13 | 89.2754 | −48 |
| 2016-12-25 | 41.2237 | −36 |
| 2017-01-06 | 24.5749 | −24 |
| 2017-01-18 | 25.7572 | −12 |
| 2017-01-30 | 0 | 0 |
| 2017-02-23 | 41.6563 | 24 |
| 2017-03-07 | 48.3596 | 36 |
| 2017-03-19 | −17.8744 | 48 |
| 2017-03-31 | 6.71604 | 60 |
| 2017-04-12 | −29.0038 | 72 |
| 2017-04-24 | 14.7846 | 84 |
| 2017-05-06 | −103.157 | 96 |
| 2017-05-18 | −71.4633 | 108 |
| 2017-05-30 | −5.27029 | 120 |
| 2017-06-11 | 12.532 | 132 |
| 2017-06-23 | 27.2988 | 144 |

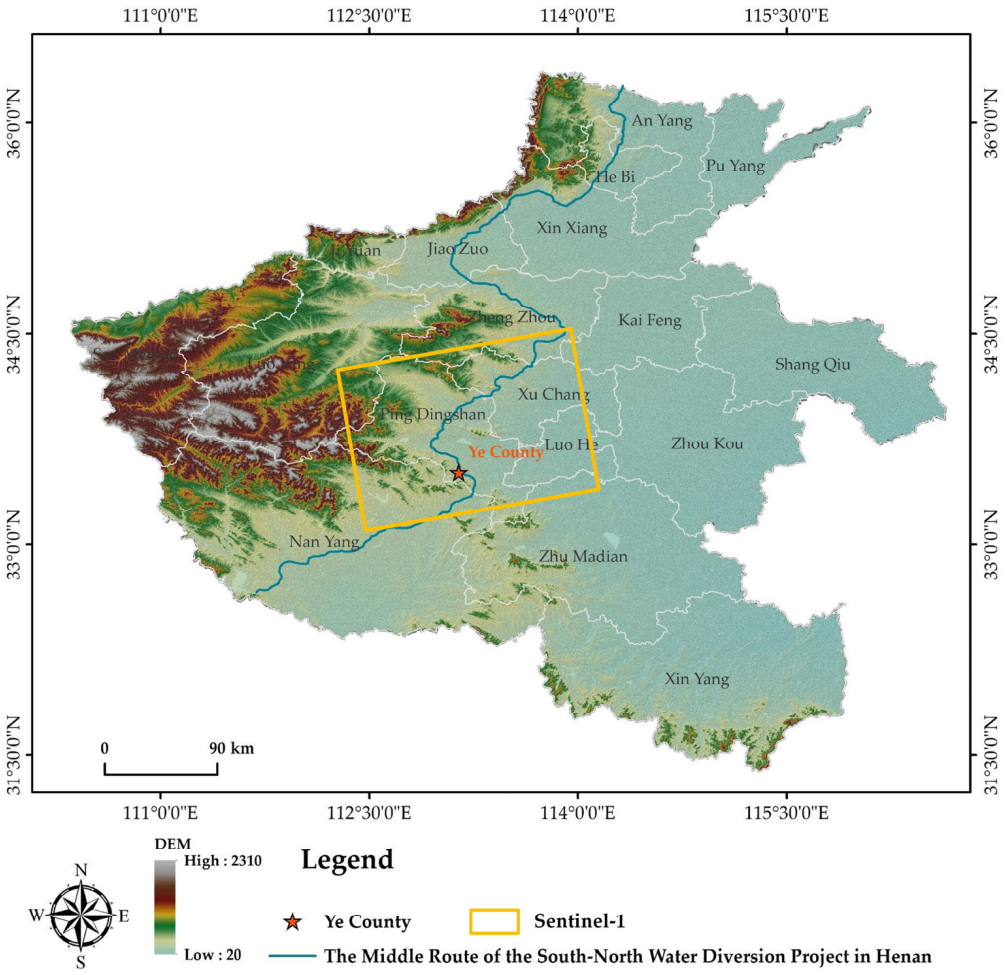


**Figure 2.** Study area DEM and coverage of SAR datasets.

The verification data use high precision second-order leveling measurement results. Figure 3a shows the second-order leveling benchmarks distributed in the road shoulder, wave wall, and other locations on both sides of the canal. There are several monitoring sections, and each section has four benchmarks. The four yellow lines represent the key monitoring sections, which can truly reflect the settlement amount and settlement trend on both sides of the high-fill canal in Wenzhuang Village, Ye County.

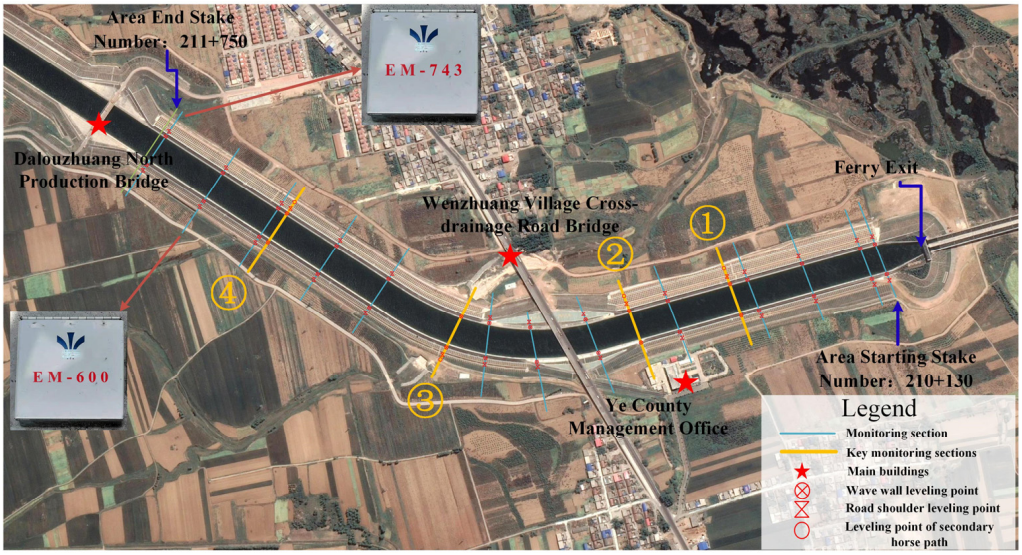


**Figure 3.** (**a**) Canal second-order leveling points location map; (**b**) Model chart of high fill; (**c**) Live aerial image. ①–④ are four key monitoring sections.

### *2.3. Research Methodology*

The PS-InSAR technique (Figure 4) selects stable points with high reflectivity in the image as PS (Persistent Scatterer) points after long time series screening. The phase information that affects the coherence of SAR images, such as terrain, atmosphere, and flatlands, is separated based on the phase information of the selected points, producing phase information that reflects significant terrain changes. The selection of permanent scatterer points uses the ratio of the standard deviation of amplitude to the mean value, the magnitude of this value determines the stability of PS points, and the points with high amplitude deviation values are experimentally selected as valid data. The value of Amplitude deviation value for identifying the selected PS points is calculated use Equation (1).

$$D_{\varphi(\mathrm{i},j)} = \frac{std[\varphi(i,j)]}{mean[\varphi(i,j)]} \leq Th, \tag{1}$$

where $D_{\varphi(\mathrm{i},j)}$ is the ratio of the standard deviation of the amplitude and the mean value of each pixel $(i,j)$ in the image; $Th$ represents the set threshold value. If $D_{\varphi(\mathrm{i},j)} \leq Th$, the pixel meets the coherence requirement, the pixel is selected as the permanent scatterer point.

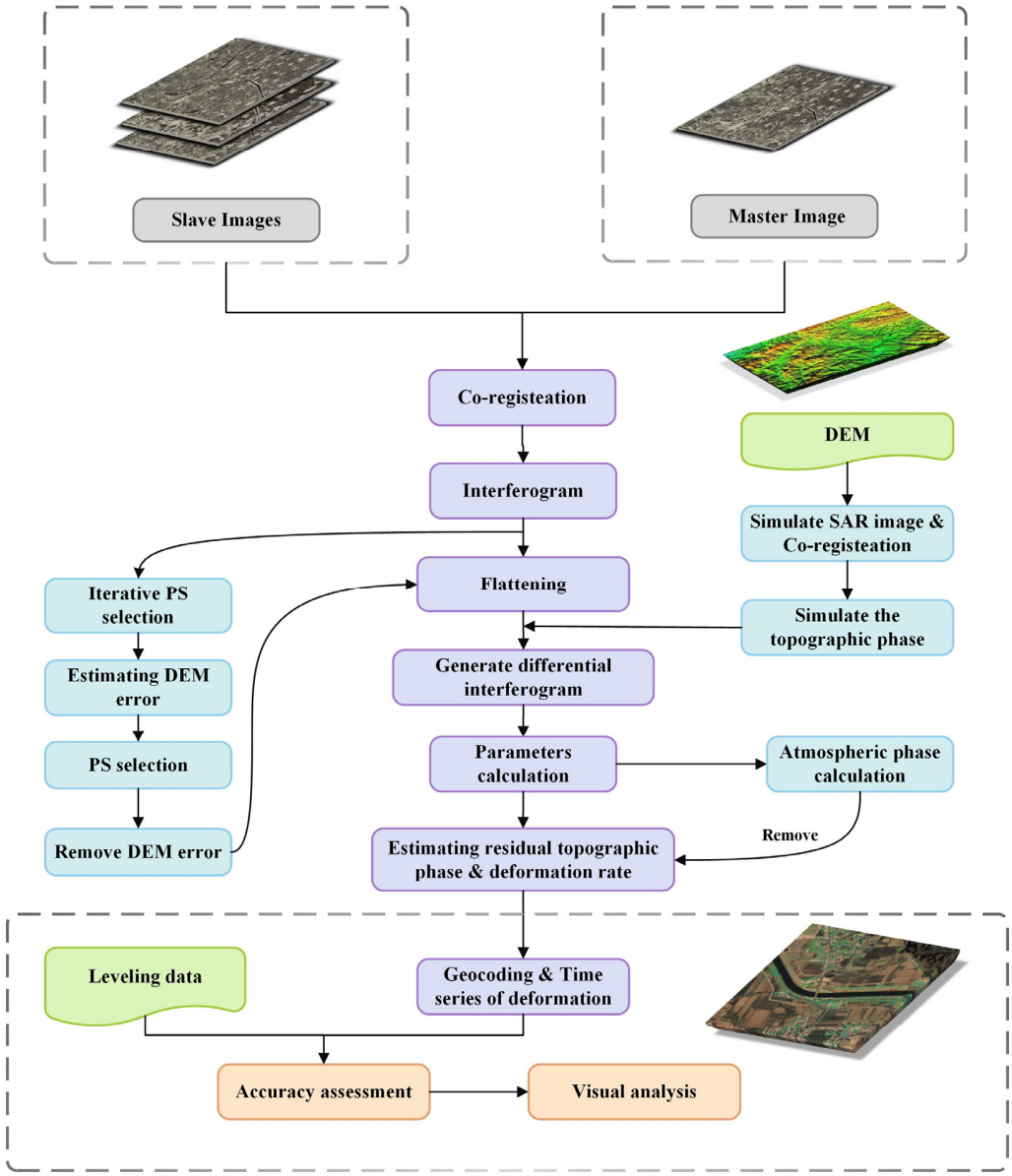


**Figure 4.** Flow chart of PS-InSAR.

The PS point phase can be expressed by Equation (2) when image alignment and interference operations are performed on master and slave images during SAR image data processing, which contains the residual elevation phase, topographic phase, noise phase, etc.

$$\varphi_{\text{int}} = \varphi_{flat} + \varphi_{def} + \varphi_{topo} + \varphi_{atm} + \varphi_{noise}, \tag{2}$$

where $\varphi_{flat}$ is the flat earth phase; $\varphi_{def}$ is the surface deformation phase in the *LOS* (Line of Sight) direction; $\varphi_{topo}$ is the introduced DEM phase difference; $\varphi_{atm}$ is the atmospheric phase difference; $\varphi_{noise}$ is the image noise phase difference. Among them, the flat earth phase, surface deformation phase, and residual terrain phase can be expressed by Equations (3)–(5), respectively.

$$\varphi_{flat} = \frac{4\pi}{\lambda R \tan\theta} B_{\perp} \Delta R, \tag{3}$$

$$\varphi_{def} = \frac{4\pi}{\lambda} T \Delta v, \tag{4}$$

$$\varphi_{topo} = \frac{4\pi}{\lambda R \sin\theta} B_{\perp} \Delta h, \tag{5}$$

where $\lambda$, $\theta$, and $R$ are the radar wavelength, incidence angle, and slope distance, respectively; $B_{\perp}$ is the spatial baseline; $T$ is the time baseline; $\Delta v$ is the $LOS$ directional deformation rate increments; $\Delta h$ is the elevation correction increments.

The interferometric phase model established above plays a major role in the linear deformation rate and elevation error, and there is spatial correlation between adjacent PS points, and the neighborhood difference model established according to two adjacent PS points is shown as Equation (6).

$$\Delta\varphi_{diff} = \frac{4\pi}{\lambda} T \Delta v + \frac{4\pi}{\lambda R \sin\theta} B_{\perp} \Delta h + \Delta w, \tag{6}$$

where $\Delta v$ is the deformation increment; $\Delta h$ is the phase elevation error increment; $\Delta w$ is the residual phase. The residual phase includes atmospheric, noise, and nonlinear phases.

The atmospheric phase and noise phase of the selected PS points in the same location and the same space tend to be close to zero, which can be neglected in the process of interference processing. If $\Delta w$ is neglected, the distribution of PS points can be connected into a mesh according to the distribution of PS points, and the deformation increment and elevation increment can be solved by Equation (6) to obtain the deformation rate field of the region of interest.

The deformation of the South–North Water Diversion Project canal obtained based on the PS-InSAR technique is the satellite line-of-sight direction deformation, which is the projection of the real deformation in the satellite line-of-sight direction. It has been shown that the deformation can be converted to the deformation in the vertical direction by using Equation (7) through the imaging geometry relationship [36], as shown in Figure 5.

$$Def_v = \frac{Def_{LOS}}{\cos\theta}, \tag{7}$$

where $\theta$ is the satellite line-of-sight to the angle of incidence; $Def_v$ is the canal vertical direction deformation variable.

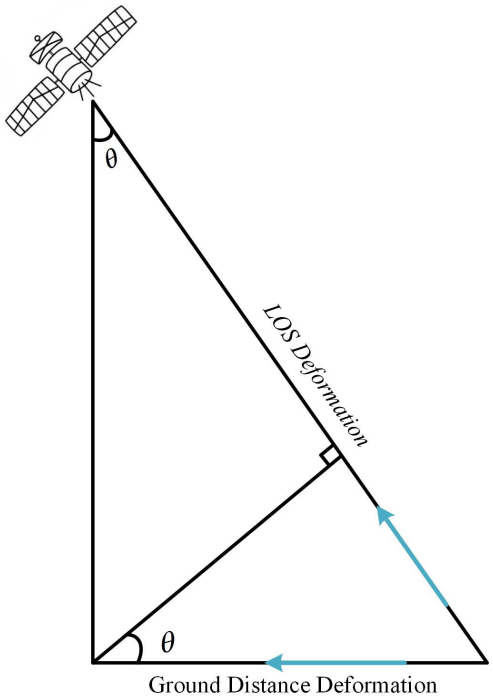


**Figure 5.** Geometric relationship between line-of-sight LOS deformation and ground distance deformation.

## 3. Data Results and Analysis

### *3.1. PS-InSAR Deformation Monitoring Results of South–North Water Diversion Project High Fill Canals*

Sentinel-1A radar images from October 2016 to June 2017 were used to monitor the deformation of the high-fill canal in Wenzhuang Village, Ye County, Middle Route of the South–North Water Diversion Project using PS-InSAR technology. The subsidence results are shown in Figure 6, and the number of extracted PS monitoring points is much larger than the density of benchmarks. There is an obvious surface deformation phenomenon in about 1 km area on the east side of the canal, and the magnitude of the deformation reached 36 mm. It can be found the deformation on the east side of the canal is more serious than that on the west side of the canal. Since the data are ascending orbit data, the satellite orbits around the polar orbit, its observation direction is the lower right side of the vertical flight direction, and the projection on the ground is nearly from west to east. Therefore, when detecting features with strong reflectivity and obvious deformation, the angle of the east side of the canal forms a nearly vertical reflection with the satellite, which is more reflective. On the contrary, the reflectivity of the west side of the canal is weaker, which has an impact on the real monitoring results.

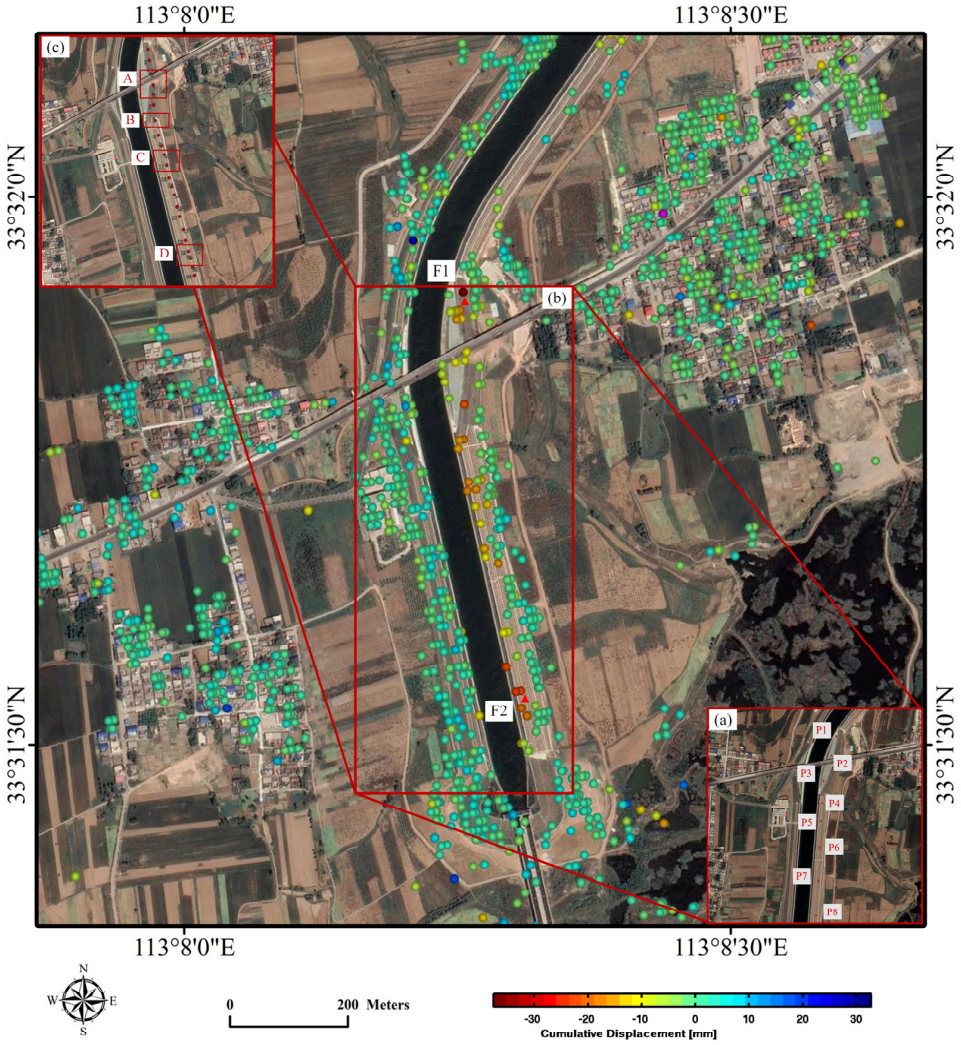


**Figure 6.** PS-InSAR deformation monitoring results of the high fill canal in Wenzhuang Village, Ye County during December 2016–June 2017 (**a**) point location map comparing PS-InSAR data with second order leveling datas; (**b**) section of canal focus area; (**c**) point location map of longitudinal section and focus deformation area.

Refined analysis of the canal in the section from pile number 210 + 130 to pile number 211 + 750 in Wenzhuang Village, Ye County, Middle Route of the South–North Water Diversion Project. There is obvious regional subsidence at F1 and F2 in Figure 6, and the causes of subsidence are divided into the following cases. The F2 monitoring point is at the exit of the ferry due to the fast flow rate of the canal, causing a small piece of serious deformation of the canal. At the location of point F1, it is located at the bend in the canal, above the bridge of the provincial highway; there are often large trucks passing through, and the speed is faster, which also causes the structure of the canal below to change easily.

### *3.2. Comparison Analysis of PS-InSAR Results and Second Order Leveling Data*

To verify the reliability of PS-InSAR technology in monitoring the slope deformation of the high-fill canal of the South–North Water Diversion Project, eight benchmarks in the study area shown in Figure 6a were selected for comparison and verification. The deformation of the PS point line of sight direction is projected onto the vertical direction according to Equation (7), and the second-order leveling data is zeroed out according to the time period. The PS-InSAR monitoring results and the time series displacement changes of the second-order leveling measurement results are shown in Figure 7. The deformation trends match perfectly, which fully proves the reliability of the PS-InSAR technique.

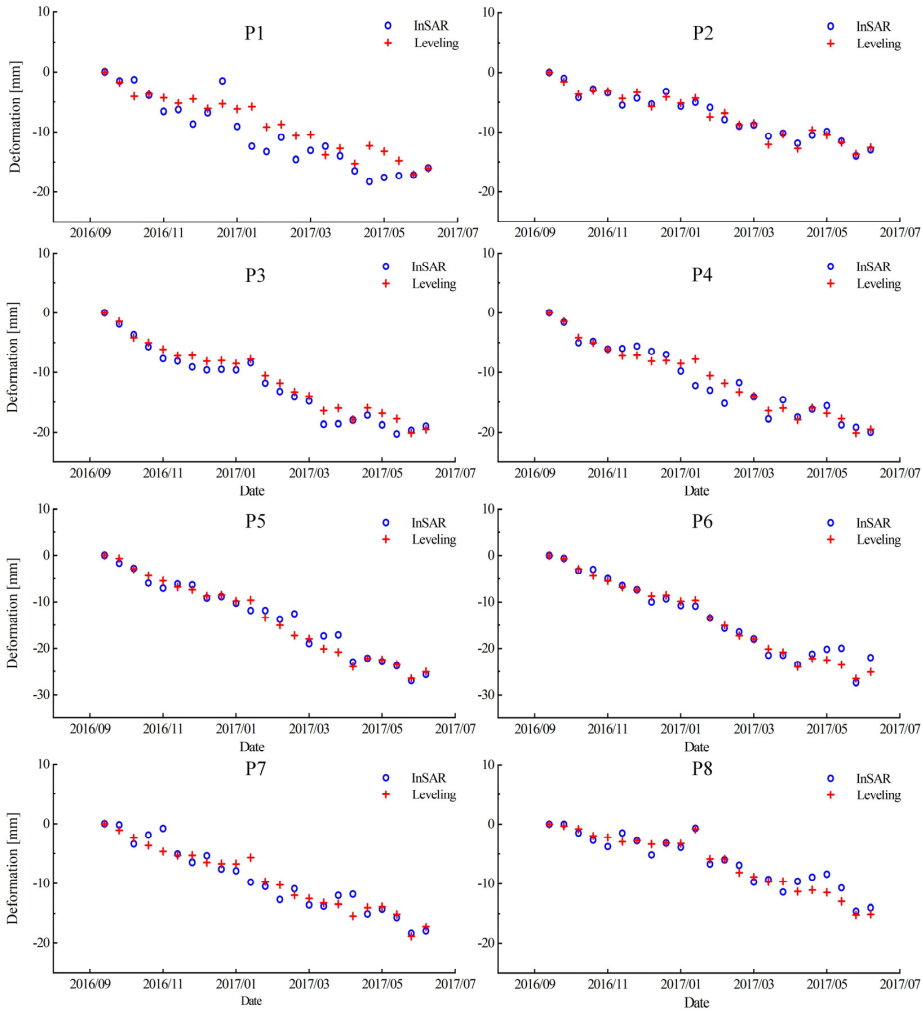


**Figure 7.** Variation of PS-InSAR monitoring results from second-order leveling measurements.

To further quantify the reliability of InSAR deformation monitoring results, Root Mean Square Error (*RMSE*) was used to evaluate the degree of agreement between InSAR results and level measurement results.

$$RMSE = \sqrt{\sum_{i=1}^{n} \Delta h_i^2 / n}, \quad (8)$$

where $\Delta h_i$ is the difference between the $i$th level data and the resultant settlement of InSAR monitoring data, and $n$ is the number of selected points.

The comparison deformation results between the benchmarks and PS points are shown in Table 2. More than 87% of RMSE values are less than ±2 mm, the maximum is 3.02 mm; the maximum value of the difference between the two is 6.59 mm. From Figure 7, it can be seen that the time that causes the large fluctuation of the P1 point appears between December 2016 and March 2017, which is mainly caused by the inconsistent matching position of the PS point and benchmark. Meanwhile, it can be found that the P1 point is located at the filling and cutting boundary of high-fill canal, as shown in Figure 3c. In the process of engineering construction, the boundary construction is poor and easy to deform. Moreover, there are three problems in the stability of high fill. First, because the soil subgrade slope of high fill is of high height and poor stability, it is easy to landslide. Second, because the high filling height is larger, it will lead to a large settlement of the foundation under the subgrade, which is easy to damage. Third, due to the high fill soil material problem, in the case of rainfall, infiltration will occur, causing instability to occur easily. Through the above three questions, combined with the position of P1, we believe that this is the reason for the difference between the analyzed values of P1 and other positions. In addition, P1 and P8 also showed strong inconsistency around May 2017. It can be seen from Figure 6 that P1 and P8 were both located in areas with serious canal subsidence. During PS-InSAR processing, the image data cycle was 12 days, which would lead to errors in monitoring values due to time incoherence. The correlation between the PS-InSAR results and the eight benchmarks results is further counted. As shown in Figure 8, the correlation coefficient reaches 0.96, and the RMSE of the difference is 1.279 mm, which is highly consistent with each other in terms of deformation trends and magnitudes. Therefore, it is sufficient to prove the reliability of the PS-InSAR results in this paper.

**Table 2.** Comparison of level results with PS-InSAR results.

| Point | RMSE/mm | Mean/mm | Maximum Difference/mm |
|---|---|---|---|
| P1 | 3.02 | 2.37 | 6.59 |
| P2 | 0.73 | 0.61 | 1.53 |
| P3 | 1.36 | 1.15 | 2.61 |
| P4 | 1.57 | 1.17 | 4.41 |
| P5 | 1.65 | 1.18 | 4.68 |
| P6 | 1.31 | 0.94 | 3.55 |
| P7 | 1.73 | 1.32 | 4.11 |
| P8 | 1.3 | 1.01 | 3.06 |

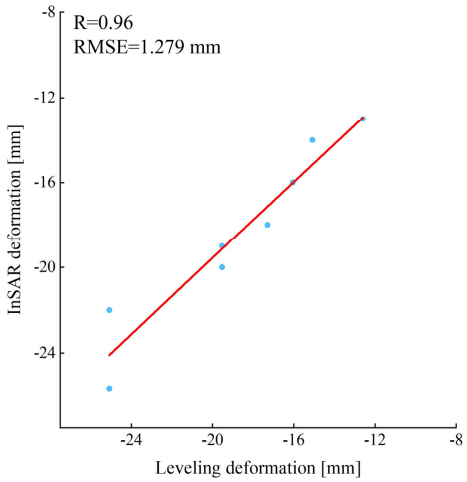


**Figure 8.** Regression analysis of level monitoring and InSAR monitoring formal variables.

### *3.3. Key Deformation Area Cross-Sectional Analysis*

Using the PS-InSAR monitoring of deformation data in two time periods, 31 March 2017 and 30 May 2017, a point was evenly selected every 50 m. The longitudinal section (along the canal direction) was analyzed for the key deformation area of about 1 km canal within Figure 6b. The point locations of longitudinal sections are shown in Figures 6c and 9, respectively. It is obvious that the locations of the four minimum points in Figure 9 correspond to Figure 6c areas A, B, C, and D, which show obvious sinking phenomena.

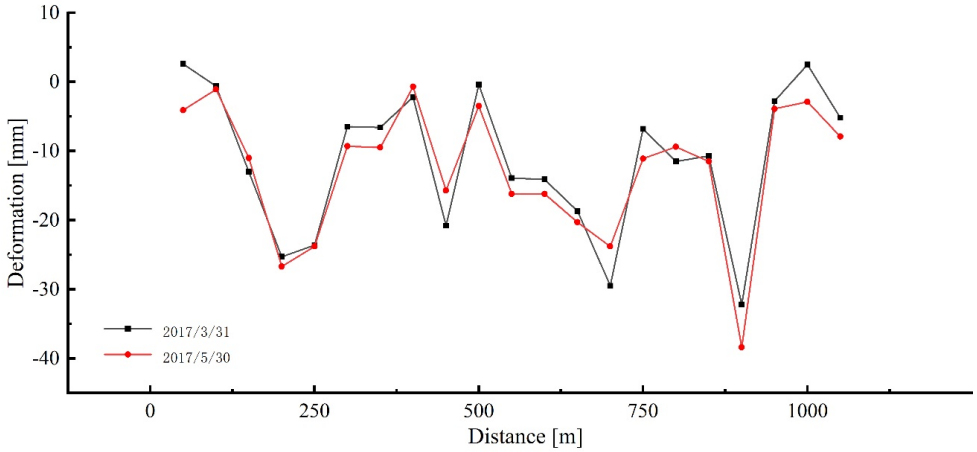


**Figure 9.** Settlement map of the longitudinal section in key deformation area.

Using the settlement in the period of 6 January 2017, the four key monitoring surfaces in Figure 3 were analyzed in cross-section (canal direction). As shown in Figure 10, the west bank of the canal is relatively stable. There are no PS points in the canal, all of them are 0 mm. The east bank of the canal shows an obvious downward trend, and the closer to the water, the larger the canal deformation is, and vice versa, the smaller it is.

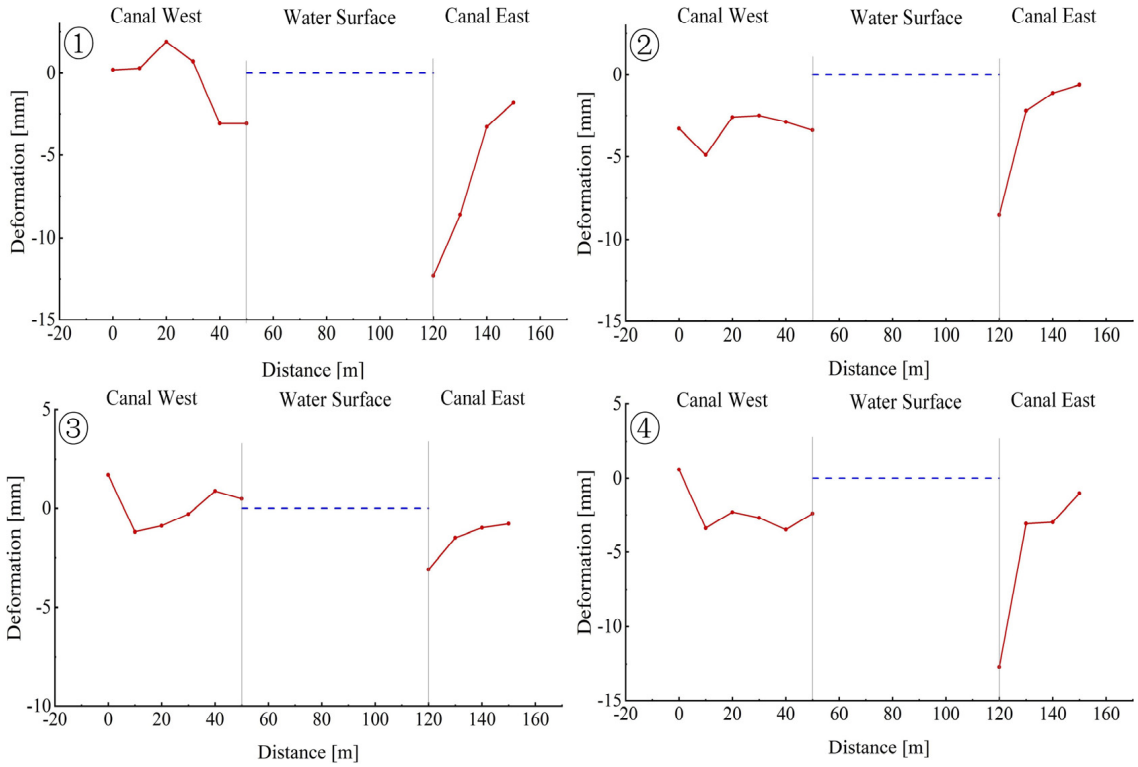


**Figure 10.** Key monitoring surface cross-sectional sedimentation map.

After 14 more images are collected, the deformation rate results of the high fill canal obtained by using PS-InSAR technology are shown in Figure 11b. The sampling time span is from October 2016 to February 2018. Compared with 11a, the shoulders and wave walls on the east and west sides of the canal show different degrees of subsidence, and the deformation on the east bank is more obvious than that of the west bank. The maximum deformation amounts to 74 mm. Therefore, the PS-InSAR technique cannot only obtain the extent and rate of settlement of the South–North Water Diversion Project Canal, but it also concludes that the east bank sinks first and the right bank sinks later.

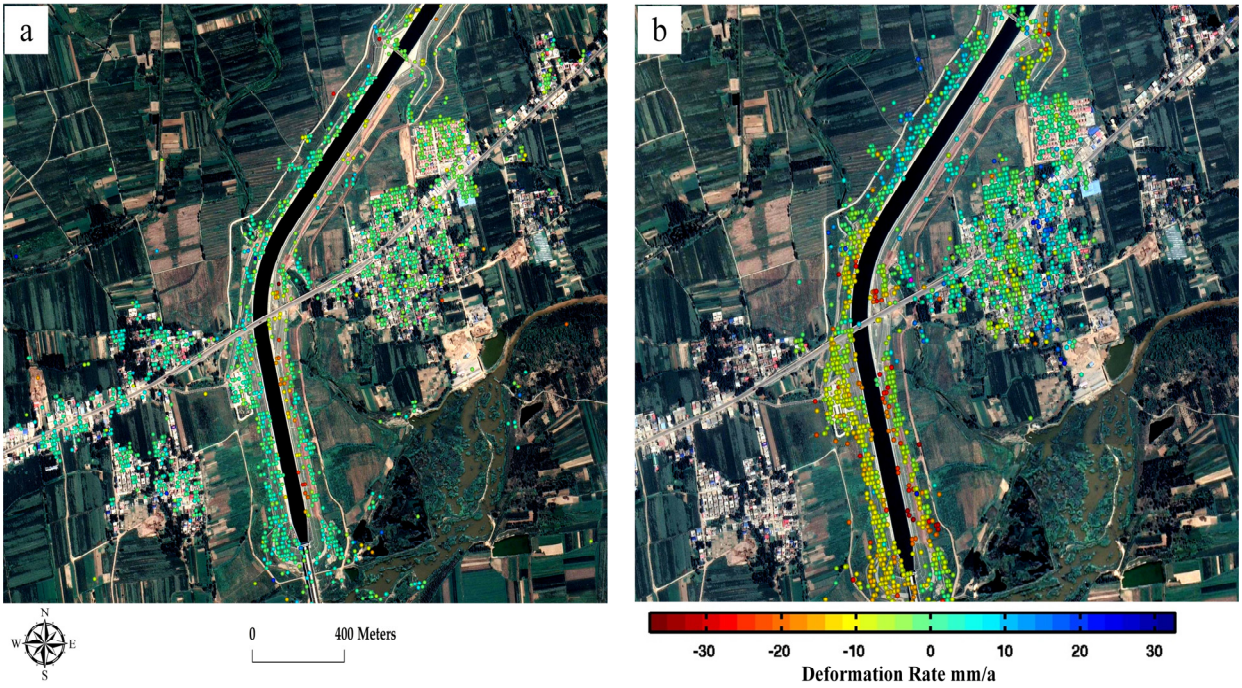


**Figure 11.** PS-InSAR deformation monitoring results of high fill canals at different periods. (**a**) December 2016–June 2017 (**b**) December 2016–February 2018.

## 4. Discussion

As a large-scale water conservancy project in China, the South–North Water Diversion Project plays an important role and safety monitoring is a key task, but due to its huge construction, a large-scale and high-precision deformation monitoring technology is urgently needed. The results of several studies show that its monitoring accuracy can reach a millimeter level, which can accurately reflect the deformation of the ground feature. Therefore, this paper uses this technology to monitor the deformation of the high-fill canal section of the South–North Water Diversion points out the areas with serious deformation and studies the feasibility of applying PS-InSAR technology to large-scale water conservancy projects.

According to the above study, it is shown that the application of PS-InSAR technology can effectively monitor the deformation of the high-fill canal of the South–North Water Diversion Project. The accuracy of PS-InSAR monitoring effect is evaluated in combination with the second order leveling data, which proves that PS-InSAR technology can provide accurate monitoring results. Compared with conventional measurements, the use of PS-InSAR technology has the advantages of high accuracy, wide range monitoring, and flexible observation. In this paper, we used PS-InSAR monitoring results to make a cross-sectional analysis of the key deformation areas of the South–North Water Diversion Canal. According to the longitudinal section analysis, the overall deformation of the canal is small. However, there are four areas with severe deformation at the same time. According to the cross-sectional analysis, the west bank of the canal is more stable, the east bank of the canal shows an obvious downward trend, and the closer to the water, the larger the canal deformation is,

and vice versa, the smaller the deformation law is. The canal can cause greater variability in the shape of the canal close to the canal due to the presence of water flow over a long period of time, while further demonstrating the reliability of the technique and realistic response to the deformation state of the canal.

The use of PS-InSAR technology can provide more means to monitor the deformation of large water conservancy projects and can analyze the deformation of water conservancy projects in all aspects, as well as the overall deformation status of key areas. No settlement occurred on the west bank of the canal during October 2016 to June 2017, and based on further processing of the collected image data, it was found that the canal also experienced settlement on the west bank over time, with greater deformation on the east bank compared to the west bank. At the same time, using PS-InSAR technology, it is possible to find out the historical deformation and the development trend of deformation and be able to make an accurate response. The study helps managers to understand the deformation characteristics and key deformation areas of the South–North Water Diversion Canal. Through systematic analysis, the settlement mechanism of the Ye County section of the Middle Route of the South–North Water Diversion Project is analyzed and the locations that need to be monitored are pointed out.

## 5. Conclusions

The Middle Route of the South–North Water Diversion Project is the "lifeline" of water supply for Beijing, Tianjin, Hebei and Henan, and the safety monitoring is of great significance. In this paper, we used the Sentinel-1A image dataset from October 2016 to June 2017 to obtain the overall deformation results of the high-fill section of Wenzhuang Village in Ye County of The Middle Route of the South–North Water Diversion Project using the time-series InSAR technique and found that the slope of about 1 km long on the east bank of the canal had obvious deformation with the maximum deformation of 36 mm. More than 87% of RMSE values are less than $\pm 2$ mm and the correlation coefficient is 0.96, which is highly consistent with the deformation trend and value, fully proving the feasibility and effectiveness of InSAR technology for the safety monitoring of the high-fill canal of the South–North Water Diversion Project. Further, using PS-InSAR technology to obtain the deformation results of the canal between October 2016 and February 2018, it was found that settlement also occurred on the west bank with time, and the deformation volume was larger on the east bank compared with the west bank. This technique can not only monitor the extent and rate of settlement in the South–North Water Diversion Canal but also accurately identify the sequence of settlement on the east and west banks, which can play an important role in monitoring the safety of large-scale linear water conservancy projects.

**Author Contributions:** H.L. and W.Z. conceived and designed the study; SAR data was processed by Z.Q.; W.Z. wrote the paper; T.W. supervised the work; G.L. and M.Z. contributed to correct the language and layout of the manuscript. All authors have read and agreed to the published version of the manuscript.

**Funding:** This work was supported by the National Natural Science Foundation of China (No.41901411), Henan Provincial Science and Technology Research Project (No.212102310052), Training Plan for Young Backbone Teachers of Colleges and Universities in Henan Province (No.2021GGJS073), Henan Province Young Talent Support Project (No.2020HYTP010), Open Foundation of Key Laboratory of Ecological Environment Protection of Space Information Application of Henan (22-FW-07-0107), and Joint Fund of Collaborative Innovation Center of Geo-Information Technology for Smart Central Plains, Henan Province and Key Laboratory of Spatiotemporal Perception and Intelligent Processing, Ministry of Natural Resources (No.211103), Major Science and Technology Special Projects in Henan Province (No.201300311400).

**Institutional Review Board Statement:** Not applicable.

**Informed Consent Statement:** Not applicable.

**Data Availability Statement:** The Sentinel-1 data used in this study is free and openly accessible to the public.

**Acknowledgments:** The authors thank the anonymous reviews for their constructive comments and suggestions.

**Conflicts of Interest:** The authors declare no conflict of interest.

## References

1. Liu, C.; Zheng, H. South-to-north Water Transfer Schemes for China. *Int. J. Water Resour. Dev.* **2002**, *18*, 453–471. [CrossRef]
2. Moore, S.M. Modernisation, authoritarianism, and the environment: The politics of China's South–North Water Transfer Project. *Environ. Politics* **2014**, *23*, 947–964. [CrossRef]
3. Office of the South-to-North Water Diversion Project Construction Committee. The South-to-North Water Diversion Project. *Engineering* **2016**, *2*, 265–267. [CrossRef]
4. Zhu, J.; Li, Z.; Jun, H. Research progress and methods of InSAR for deformation monitoring. *Acta Geod. Cartogr. Sin.* **2017**, *46*, 1717–1733. [CrossRef]
5. Zhang, L.; Lu, Z. Advances in InSAR Imaging and Data Processing. *Remote Sens.* **2022**, *14*, 4307. [CrossRef]
6. Biggs, J.; Wright, T.J. How satellite InSAR has grown from opportunistic science to routine monitoring over the last decade. *Nat. Commun.* **2020**, *11*, 3863. [CrossRef] [PubMed]
7. Wang, T.; Perissin, D.; Rocca, F.; Liao, M.-S. Three Gorges Dam stability monitoring with time-series InSAR image analysis. *Sci. China Earth Sci.* **2010**, *54*, 720–732. [CrossRef]
8. Liu, W.; Liu, H.; Song, Z.; Hu, Q. Research on the training mode of water conservancy talents with surveying and mapping background in the new era. *J. N. China Univ. Water Resour. Electr. Power (Soc. Sci. Ed.)* **2022**, *43*, 1–10. [CrossRef]
9. Liu, H.; Xu, Q. Interference processing for zero intermediate frequency multi-baseline InSAR sssisted by DEM. *J. Henan Norm. Univ. (Nat. Sci. Ed.)* **2018**, *46*, 42–47. [CrossRef]
10. Zhang, P.; Guo, Z.; Guo, S.; Xia, J. Land Subsidence Monitoring Method in Regions of Variable Radar Reflection Characteristics by Integrating PS-InSAR and SBAS-InSAR Techniques. *Remote Sens.* **2022**, *14*, 3265. [CrossRef]
11. Liu, H.; Jin, G.; Zhang, H.; Xu, Q. DEM assisted zero intermediate frequency baseline estimation method of InSAR. *J. Huazhong Univ. Sci. Technol. (Nat. Sci. Ed.)* **2017**, *45*, 79–84. [CrossRef]
12. Xiang, W.; Zhang, R.; Liu, G.; Wang, X.; Mao, W.; Zhang, B.; Fu, Y.; Wu, T. Saline-Soil Deformation Extraction Based on an Improved Time-Series InSAR Approach. *ISPRS Int. J. Geo-Inf.* **2021**, *10*, 112. [CrossRef]
13. Ferretti, A.; Prati, C. Nonlinear subsidence rate estimation using permanent scatterers in differential SAR interferometry. *IEEE Trans. Geosci. Remote Sens.* **2000**, *38*, 2202–2212. [CrossRef]
14. Ferretti, A.; Fumagalli, A.; Novali, F.; Prati, C.; Rocca, F.; Rucci, A. A New Algorithm for Processing Interferometric Data-Stacks: SqueeSAR. *IEEE Trans. Geosci. Remote Sens.* **2011**, *49*, 3460–3470. [CrossRef]
15. Zhu, X.X.; Bamler, R. Super-Resolution Power and Robustness of Compressive Sensing for Spectral Estimation With Application to Spaceborne Tomographic SAR. *IEEE Trans. Geosci. Remote Sens.* **2012**, *50*, 247–258. [CrossRef]
16. Liu, H.; Yue, J.; Huang, Q.; Li, G.; Liu, M. A Novel Branch and Bound Pure Integer Programming Phase Unwrapping Algorithm for Dual-Baseline InSAR. *Front. Environ. Sci.* **2022**, *10*, 890343. [CrossRef]
17. Ma, P.; Lin, H. Robust Detection of Single and Double Persistent Scatterers in Urban Built Environments. *IEEE Trans. Geosci. Remote Sens.* **2016**, *54*, 2124–2139. [CrossRef]
18. Del Soldato, M.; Solari, L.; Raspini, F.; Bianchini, S.; Ciampalini, A.; Montalti, R.; Ferretti, A.; Pellegrineschi, V.; Casagli, N. Monitoring Ground Instabilities Using SAR Satellite Data: A Practical Approach. *ISPRS Int. J. Geo-Inf.* **2019**, *8*, 307. [CrossRef]
19. Liu, H.; Li, G.; Xu, Q.; Lou, L. Inclination angle error compensation algorithm of MIMO downward looking array SAR. *Acta Geod. Cartogr. Sin.* **2018**, *47*, 973–985. [CrossRef]
20. Rouet-Leduc, B.; Jolivet, R.; Dalaison, M.; Johnson, P.A.; Hulbert, C. Autonomous extraction of millimeter-scale deformation in InSAR time series using deep learning. *Nat. Commun.* **2021**, *12*, 6480. [CrossRef]
21. Liu, H.; Li, G.; Jin, G.; Xu, Q. Array vibrating error compensation algorithm of MIMO downward-looking array SAR. *J. Geomat. Sci. Technol.* **2018**, *35*, 175–181.
22. Lyu, M.; Ke, Y.; Guo, L.; Li, X.; Zhu, L.; Gong, H.; Constantinos, C. Change in regional land subsidence in Beijing after south-to-north water diversion project observed using satellite radar interferometry. *GIScience Remote Sens.* **2019**, *57*, 140–156. [CrossRef]
23. Ghorbani, Z.; Khosravi, A.; Maghsoudi, Y.; Mojtahedi, F.F.; Javadnia, E.; Nazari, A. Use of InSAR data for measuring land subsidence induced by groundwater withdrawal and climate change in Ardabil Plain, Iran. *Sci. Rep.* **2022**, *12*, 13998. [CrossRef] [PubMed]
24. Bai, Z.; Wang, Y.; Balz, T. Beijing Land Subsidence Revealed Using PS-InSAR with Long Time Series TerraSAR-X SAR Data. *Remote Sens.* **2022**, *14*, 2529. [CrossRef]
25. Dai, K.; Deng, J.; Xu, Q.; Li, Z.; Shi, X.; Hancock, C.; Wen, N.; Zhang, L.; Zhuo, G. Interpretation and sensitivity analysis of the InSAR line of sight displacements in landslide measurements. *GIScience Remote Sens.* **2022**, *59*, 1226–1242. [CrossRef]

26. Huang, Q.; Wang, Y.; Xu, J.; Nishyirimbere, A.; Li, Z. Geo-Hazard Detection and Monitoring Using SAR and Optical Images in a Snow-Covered Area: The Menyuan (China) Test Site. *ISPRS Int. J. Geo-Inf.* **2017**, *6*, 293. [CrossRef]
27. Zheng, X.; He, G.; Wang, S.; Wang, Y.; Wang, G.; Yang, Z.; Yu, J.; Wang, N. Comparison of Machine Learning Methods for Potential Active Landslide Hazards Identification with Multi-Source Data. *ISPRS Int. J. Geo-Inf.* **2021**, *10*, 253. [CrossRef]
28. Su, X.; Zhang, Y.; Meng, X.; Rehman, M.U.; Khalid, Z.; Yue, D. Updating Inventory, Deformation, and Development Characteristics of Landslides in Hunza Valley, NW Karakoram, Pakistan by SBAS-InSAR. *Remote Sens.* **2022**, *14*, 4907. [CrossRef]
29. Mohammadimanesh, F.; Salehi, B.; Mahdianpari, M.; English, J.; Chamberland, J.; Alasset, P.-J. Monitoring surface changes in discontinuous permafrost terrain using small baseline SAR interferometry, object-based classification, and geological features: A case study from Mayo, Yukon Territory, Canada. *GIScience Remote Sens.* **2018**, *56*, 485–510. [CrossRef]
30. Beck, I.; Ludwig, R.; Bernier, M.; Strozzi, T.; Boike, J. Vertical movements of frost mounds in subarctic permafrost regions analyzed using geodetic survey and satellite interferometry. *Earth Surf. Dyn.* **2015**, *3*, 409–421. [CrossRef]
31. Zhou, H.; Zhao, L.; Wang, L.; Xing, Z.; Zou, D.; Hu, G.; Xie, C.; Pang, Q.; Liu, G.; Du, E.; et al. Characteristics of Freeze–Thaw Cycles in an Endorheic Basin on the Qinghai-Tibet Plateau Based on SBAS-InSAR Technology. *Remote Sens.* **2022**, *14*, 3168. [CrossRef]
32. Dong, J.; Lai, S.; Wang, N.; Wang, Y.; Zhang, L.; Liao, M. Multi-scale deformation monitoring with Sentinel-1 InSAR analyses along the Middle Route of the South-North Water Diversion Project in China. *Int. J. Appl. Earth Obs. Geoinf.* **2021**, *100*, 102324. [CrossRef]
33. Wang, N.; Dong, J.; Wang, Z.; Lei, J.; Zhang, L.; Liao, M. Monitoring Large-Scale Hydraulic Engineering Using Sentinel-1 InSAR: A Case Study of China's South-to-North Water Diversion Middle Route Project. *IEEE J. Sel. Top. Appl. Earth Obs. Remote Sens.* **2022**, *15*, 739–750. [CrossRef]
34. Ma, C.; Qu, C.; Meng, X. Embankment stability of the north henan section of middle route project(MRP) of south-to-north water diversion based on InSAR tine series analysis. *Seismol. Geol.* **2014**, *36*, 749–762. [CrossRef]
35. Zhang, Y.; Tian, F.; Li, Y.; Liu, H. Application of time series InSAR to deformation monitoring in central line project of South-to-North Water transfer. *J. Yangtze River Sci. Res. Inst.* **2021**, *38*, 72–77. [CrossRef]
36. He, Z.; Yu, H.; Xie, S. Deformation monitoring of Xiaolangdi dam based on SBAS-InSAR technology. *Sci. Surv. Mapp.* **2022**, *47*, 66–72+82. [CrossRef]